Enhanced biosorption of Sb(III) onto living Rhodotorula mucilaginosa strain DJHN070401

Jin, Chang-sheng; Deng, Ren-jian; Ren, Bo-zhi; Hou, Bao-lin; Hursthouse, Andrew S.

Published in:
Current Microbiology

DOI:
10.1007/s00284-020-02025-z

E-pub ahead of print: 30/05/2020

Document Version
Peer reviewed version

Enhanced Biosorption of Sb(III) onto Living Rhodotorula mucilaginosa Strain DJHN070401

Jin, Chang-Sheng; Deng, Ren-Jian; Ren, Bo-Zhi; Hou, Bao-Lin; Hursthouse, Andrew S

Published in:
Current Microbiology

DOI:
10.1007/s00284-020-02025-z

E-pub ahead of print: 30/05/2020

Document Version
Peer reviewed version

Enhanced biosorption of Sb(III) onto living *Rhodotorula mucilaginosa* Strain DJHN070401: optimization and mechanism

Changsheng Jin[1], Renjian Deng[1]*, Bozhi Ren[1, 2], Baolin Hou[1, 2] and Andrew S. Hursthouse[1, 2, 3]

[1] School of Civil Engineering, Hunan University of Science and Technology; Xiangtan 411201, China

[2] Hunan Provincial Key Laboratory of Shale Gas Resource Utilization, Xiangtan 411201, China;

[3] School of Computing, Engineering & Physical Sciences, University of the West of Scotland, Paisley PA1 2BE, UK

***** Correspondence: 800912deng@sina.com

Abstract

Response surface methodology was employed to optimize a total of 13 factors to optimize biosorption of Sb(III) onto living *Rhodotorula mucilaginosa* DJHN070401. The mechanism of biosorption and bioaccumulation was also studied. The results showed biosorption reached 56.83% under the optimum conditions. In addition, pH, Fe^{2+} and temperature are significant influencing factors , and control of Ca^{2+} and Fe^{2+} has beneficial impact on Sb(III) biosorption. The characterization explained that physical adsorption occurred readily on the loose and porous surface of DJHN070401 where carboxyl, amidogen, phosphate group, and polysaccharide C-O functional groups facilitated absorption by complexation with Sb(III), accompanied by ion exchange of Na^{+}, Ca^{2+} ions with Sb(III). It was also noted thatthe growing cell not only improved the

removal efficiency in the presence of metabolic inhibitors, but also prevented intracellular Sb(III) being re-released into environment. The results of this study underpin improved and efficient methodology for biosorption of Sb(III) from wastewater.

Keywords

Rhodotorula mucilaginosa DJHN070401; enhanced biosorption; response surface method; Sb(III); mechanism

1. Introduction

Antimony (Sb) is a metalloid belonging to the same group of the periodic Tab. as arsenic, it has genetic toxicicity in human and wider biological environment and is identified to be carcinogenic (Herath et al., 2017). Together with the characteristics of strong mobility and complexation reactions in water and sediments (Henckens et al., 2016), antimony and its compounds were ranked with the priority controlled contamination in many countries (Macgregor et al., 2015). However, as a non-renewable strategic metal, Sb is widely applied to many areas, including flame retardants, metal alloy, semiconductors, pigment and therapeutic agents against protozoan disease (He et al., 2019). Therefore, a large number of antimony containing compounds enter the aquatic environment each year from various sources. China is the largest Sb producer in the world with 114 Sb mines and approximately 90% of the world's production (He et al., 2019; He et al., 2014). Long-term mining activities have caused a continuous increase in Sb concentrations in water and soils near the ore extraction and smelter areas on these sites with, Sb concentration in surface water near the Xikuangshan site in Hunan China was as high as 6 384 μg/L (He

et al., 2014), grossly exceeding the value specified by the World Health Organization and the Chinese drinking water limit (5 μg/L). Therefore, the removal of Sb from water is an important environmental problem affecting people's well-being near many antimony mines in China (Urík et al., 2019). In recent years, traditional treatment technologies have been proposed and used to remove Sb from aqueous solution, including coagulative precipitation, oxidation, electrochemical precipitation, ion exchange and membrane filtration (Ungureanu et al., 2015; Henckens et al., 2016). Although these technologies play a positive role, they still have some defects such as low efficiency, high cost, complicated operation and potential for secondary pollution (Li et al., 2018; Herath et al., 2017). Therefore, new technologies with low cost, eco-friendly materials and simple and effective application is urgently needed to reduce the environmental burdens of this contamination (Deng et al., 2017; Ungureanu et al., 2015).

In various biological processes, antimony inhibits the activity of enzymes or interferes with the metabolism of protein and sugar by irreversibly binding to intracellular sulfhydryl (-SH) group, thus toxic to living organisms (Li et al., 2018). In addition, Sb also inhibits DNA replication and cell metabolism, causing apoptosis (Banerjee et al., 2018). However, some indigenous microorganisms can able to survive under extremely high Sb concentrations stress, and even provide energy for cell growth through adsorption, redox and methylation of antimony (Li et al., 2018; Sun et al., 2016). These activities and functions are considered as a potential benefit in the remediation of soil and water contamination by antimony (Herath et al., 2017; Deng et al., 2018). Lialikova (1974) for the first time reported an antimony-oxidizing bacteria *Stibiobacter senarmontii* which opened up a research front on the interaction between microorganisms and antimony. Since then, many kinds of antimony-resistant microorganism, such as

Sphaerotilus natans (Li et al., 2018), sulfate-reducing bacteria (SRB) (Zhang et al., 2016; Wang et al., 2013), aerobic granular sludge-bacteria (Wang et al., 2014; Wan et al., 2014), *Bacillus cereus* (Li et al., 2012), cyanobacteria *Microcystis* (Vijayaraghavan and Balasubramanian, 2011; Wu et al., 2012; He and Chen, 2014) and other microorganisms (Li et al., 2013; Nguyen et al., 2017), are found to have the potential to remove Sb from aqueous solution. Most notably, bioleaching by filamentous fungi is advantageous over bacterial action because of its higher efficiency, with the ability of growth over a wide pH range and resistance to high concentration of toxic metals (Wang et al., 2014; Li et al., 2013; Deng et al., 2018; Wang et al., 2019). However, it is rarely reported the biosorption by living fungi can be used to remove antimony from water. Consequently, fundamental understanding of theoretical process of biosorption of Sb(III) onto living fungi is not clear. It is generally known that microbial growth environment is one of the most significant factors affecting microbial adsorption capacity and properties (Li et al., 2013; Deng et al., 2018). Hence, in order to attain the maximum removal rate of living fungi systems, it is crucial to find the maximum fungi production yield, requiring detailed understanding of the significance of influencing factors (carbon source, pH, inorganic matter, etc.) of fungal culturing and the adsorption process (Wan et al., 2014; Ungureanu et al., 2015). In addition, to identify and understand the complexity of the metal biosorption process, it is critical to recognize the interactive effects of the factors along with the individual effects of the experimental factors (Jaafari and Yaghmaeian, 2019). Response surface methodology (RSM) is a useful model to simultaneously study the relationships existing between the effects of several individual factors influencing the responses by varying these factors simultaneously (Jaafari and Yaghmaeian, 2019; Reddy et al., 2008). Moreover, mastering functional mechanisms of adsorption removal heavy

metals has contributed to develop desirable microbial strain resources. The current research generally assumes that the mechanism of antimony removal by microorganism is mainly complexation and ion exchange (Wang et al., 2014; Wu et al., 2012; Uluozlu et al., 2010; Zhang et al., 2011), while the adsorption mechanisms of Sb(III)/Sb(V) by iron salts is redox and ion exchange (Mittal et al., 2013; Guo et al., 2014; Xu et al., 2011). However, there is little clarity on the mechanistic interaction between fungi, iron salts and Sb(III) or Sb(V), their interactions, the migration and transformation processes of antimony between water and adsorbents, and adsorption mechanism have not been reported.

In this paper, the response surface methodology (RSM) is used to optimize the culture conditions and adsorption parameters of *Rhodotorula mucilaginosa* DJHN070401 obtained in our previous research. The significant influencing factors and their interaction effects in the removal of Sb(III) were determined. The biosorption mechanisms of the living DJHN070401 were characterized and determined by modern characterization techniques. Finally, in order to confirm that removal of Sb(III) into DJHN070401 in this study is due to biosorption, the effect of DCC (N,N'-dicyclohexylcarbodiimide, specific ATPase inhibitor) activities on the biosorption efficiency of Sb(III) and re-release of intracellular Sb(III) into the environment were studied (Luo et al., 2011). This paper presents an enhanced biosorption removal method with potential applications in engineering for better prevention and control of antimony pollution.

2. Materials and methods

2.1. Isolation and culture conditions of *Rhodotorula mucilaginosa* DJHN070401

Rhodotorula mucilaginosa DJHN070401 (MH611511) was isolated from a soil sample with high Sb content. Because of its ability to produce characteristic carotenoids (torulene, torularhodin, γ-carotene and β-carotene), *Rhodotorula* play an important role in aquaculture and in purifying the water environment (Bhosale and Gadre, 2001). DJHN070401 was inoculated into 9K liquid medium and activated for 24 h. Then, the fungus suspension was inoculated into fresh beef extract peptone liquid medium by 5% inoculation dose to obtain a certain concentration of the fungus suspension (Li et al., 2013). Then, it was stored in a refrigerator at 4 °C before use.

2.2. Establishing response surface methodology

2.2.1. Single factor test

The effects of nutritional and environmental factors on biomass yield and Sb(III) removal efficiency of the DJHN070401 strain were investigated using single factor test (Jaafari and Yaghmaeian, 2019; Reddy et al., 2008). As shown in Table S1, total of seven nutritional factors (carbon source and concentration, nitrogen source and concentration, Fe^{2+} concentration, inorganic salt and inorganic salt concentration) (Bhagwat et al., 2014), as well as total of six environmental factors (initial pH, temperature, agitation speed, inoculation dose, initial Sb(III) concentration and adsorption time), were taken to identify the best growth factors and adsorption condition for strain DJHN070401.

Single factor test was carried out by batch experiments. To investigate the influence of carbon source, 2%(v/v) fungus suspension was inoculated into the beef extract peptone liquid medium with different carbon sources (with other factors remaining constant), cultured at 30±0.5°C and 150 r/min for 48h, 20 ml of the fungus liquid was centrifuged

at 3000 r/min for 20 min, then the biomass was collected and dried in a 60°C thermostat drying box to a constant weight (Zaki et al., 2008). The fungus liquid cultured above was inoculated into the fresh beef extract peptone liquid medium with Sb(III) concentration of 10 mg/L for 24 hours at a 5% inoculation dose, and 20 ml of the sample was centrifuged at 8000 rpm for 10 min to determine residual concentration of Sb(III) in the supernatant (Xi et al., 2011). The biosorption removal rate of Sb(III) was determined by the Eq. (1).

$$R = \frac{C_0 - C}{C_0} \times 100\% \quad (1)$$

Where: *R*-the biosorption removal rate by DJHN070401 of Sb(III) (%); C_0 and *C*-the initial and adsorption equilibrium concentration of Sb(III) (mg/L), respectively.

2.2.2. Plackett-Burman experiment

On the basis of single factor testing results, the factors influencing biomass yield and Sb(III) removal rate were further investigated using the Plackett-Burman experiment. As shown in Table S2, eight influencing factors, including carbon source (glucose), pH, temperature, agitation speed, inoculation dose, Fe^{2+}, nitrogen source (beef extract and peptone) and $CaCl_2$, were selected as the research objects and divided into two levels as -1 and +1 (Jaafari and Yaghmaeian, 2019).

2.2.3. response surface methodology (RSM)

The central composite design (CCD), which was the standard RSM, was employed to enhance biosorption of Sb(III). According the results of Plackett-Burman experiment, three independent variables, i.e. Fe^{2+} concentration (1.06-1.74 mg/L), pH (3.16-4.84) and temperature (24-30°C) were taken to obtain the response on Sb(III) biosorption removal rate and biomass yield and their interaction (Jaafari and Yaghmaeian, 2019). The complete design consisted of six runs of steepest ascent tests (Reddy et al., 2008) and

twenty runs of CCD and these were performed in triplicate to optimize the levels of the selected variables. The experimental range of each variable (maximum and minimum) and levels (Reddy et al., 2008) of independent variables were considered by CCD and are presented in Table S3. The biosorption removal rate of Sb(III) (*Y*, %) was considered as the dependent factor (response). The independent parameters and the dependent output response were modeled and optimized using analysis of variance (ANOVA) to justify the adequacy of the models by *R* software RSM package(Jaafari and Yaghmaeian, 2019). The quadratic equation model for predicting the optimal conditions can be expressed as Eq. (2).

$$Yi = \beta_0 + \sum \beta_i x_i + \sum \beta_{ii} x_i^2 + \sum \beta_{ij} x_i x_j + \varepsilon \quad (2)$$

Where: *Y* is the predicted response of biosorption removal rate of Sb(III) in actual units.

2.3. Biosorption of Sb(III) by growing DJHN070401 with/without metabolic inhibitors

Based on the methods modified by Luo et al. (2011), the effect of industrially used metabolic inhibitors DCC on the efficiency of biosorption removal of Sb(III) by DJHN070401 was assessed. A 5 mL aliquot of cells was withdrawn from exponentially homogenous culture of DJHN070401 and inoculated into 100 mL freshly prepared liquid beef extract peptone medium in 250 mL conical flasks containing 15 mg/L Sb(III), 15 mg/L Sb(III) and DCC (0.5 mM), respectively. 10 mL samples were taken from the culture flasks at predefined time intervals (0, 6, 12, 18, 24 and 30 h) harvested by centrifugation (6000 r/min, 20 min, 4 ℃). The Sb(III) concentration of supernatant was analyzed to determine the biosorption removal rate of Sb(III) onto DJHN070401.

2.4. Characterization of DJHN070401 before and after adsorption of Sb(III)

The medium from each culture was centrifuged at 5000 rpm for 1 min to collect the before and after adsorption of Sb(III) biological samples. All samples were air-dried in a desiccator at ambient temperature (25 °C) (Fan et al., 2016). The samples were coated with Pt prior to the field emission-scanning electron microscope (SEM, HITACHI-S4800, Japan) analysis. Elemental components of the samples were analyzed by energy dispersive X-ray spectroscopy (EDS, XFlash 5010, Burker, German). Surface functional groups of the DJHN070401 were tested by fourier transform infrared spectroscopy (FTIR, Nicolet 6700, USA) with KBr pellets and a resolution of 1 cm^{-1} in the range of wave numbers in the range of 4000-400 cm^{-1}. X-ray diffraction (XRD, D8 Advance, AXS, German) was utilized to analyze the compounds present in the precipitate before and after adsorption of Sb(III) by DJHN070401 with Cu Kα radiation (λ=1.5418Å) operating at 40 kV and 40 mA (Guo et al., 2014). The identification of the crystalline was obtained using the X'pert High Score Plus software with PDF-4+ and ICDD datebase.

2.5. Reagents and chemcial analysis

Standard stock solution of Sb(III) of 1 g/L was prepared by dissolving $C_8H_4K_2O_{12}Sb_2$ into the deionized water. The reagents used in the experiment are analytical pure or superior pure reagents, and the experimental water is deionized water.

Hydride generation atomic fluorescence spectrometry（HG-AFS, AF-9600, Beijing Kechuang Haiguang Instrument Co., Ltd., China） was utilized to determine the concentrations of Sb(III) and Sb(V), following the method of Xi et al. (2011). The minimum detection concentration of this method was 1 μg L^{-1}. All samples were measured within one day after the adsorption experiment, and deionized water was used

for the blank. Sb(III) recovery using this test was over 95.0%. Relative standard deviations (RSDs) of duplicated samples in solution were less than 7%. For each input concentration C_0, the tests were performed in triplicates and the mean and standard error (SE) of the amount of Sb(III) and Sb_{tot} adsorbed was reported.

3. Results and discussion

3.1. Effect of nutritional and environmental factors on Sb(III) biosorption

Both nutritional and environmental factors can significantly affect the antimony removal by biosorption of microorganisms (Wang et al., 2013; Deng et al., 2018). The results showed that the nutritional factors as carbon source, nitrogen source, inorganic salt concentration and Fe^{2+} concentration had a great influence on the growth and Sb(III) adsorption behavior of DJHN070401 (Fig.1(a~d), while carbon source concentration, nitrogen source concentration and inorganic salt had little influence on them (Fig.S1(a-c)). Glucose as its carbon source, both of the biomass and biosorption removal rate reached their maximum values of 7.56 g/L and 16.87% (Fig.1(a)), respectively. Compared with without carbon source, they were up 417.81% and 132.69%. Therefore, glucose was selected as the best carbon for both DJHN070401 growth and biosorption Sb(III).

It can be observed in Fig.1(b) that the best nitrogen source was 0.75% beef extract and 0.75% peptone, biosorption reached a removal rate for Sb(III) of 19.47%. It is generally known that iron salts, which have potential benefits in the treatment of antimony pollution (Deng et al., 2017), provide an essential nutrient element for microbial growth. In addition, yeast is a natural carrier with the ability to efficiently enrich the Fe^{2+} ion (Shin

et al., 2001). Therefore, $FeSO_4 \cdot 7H_2O$ was added to the culture medium to promote the microbial growth and biosorption of Sb(III) by DJHN070401. As expected, both the biomass and removal of Sb(III) by biosorption increased at first and then decreased with an increase in Fe^{2+} concentration(Fig.1(c)). When the Fe^{2+} concentration was in the ranged 0.2 to 1.2 g/L, the biomass changed very little (8.45~9.21 g/L), but the maximum removal of Sb(III) reached 29.35% at a concentration of 1.2 g/L Fe^{2+}. As shown in Fig. S1 (c), other inorganic salts such as $MgSO_4 \cdot 7H_2O$, $CaCl_2$, KCl, $K_2HPO_4 \cdot 3H_2O$ and KH_2PO_4 had little effect on the biomass, but did influence the removal of Sb(III) . It is worth noting that removal by biosorption reached the highest value of 40.50 % at a $CaCl_2$ concentration of 0.5% (Fig. 1 (c)). Therefore, an increase in the $CaCl_2$ concentration can promote the Sb(III) biosorption removal of DJHN070401.

As shown in Fig.1(E), as the pH value ranges from 1.0 to 10.0, both biomass and biosorption removal of Sb(III) shows an initial increase and then decreases, but with different optimal pH. The biomass of DJHN070401 reaches the maximum value of 9.66 g/L at pH 5.0 and also grows well at pH 5.0~8.0 with above 7.58 g/L of biomass generated. While the optimal pH range for Sb(III) biosorption by DJHN070401 is 3.0-4.0 with 51.77-52.73% of biosorption removal rate which is consistent with most microorganisms adsorb antimony at the optimum pH value of 3.0-6.0 (Wang et al., 2014; Wan et al., 2014; Vijayaraghavan and Balasubramanian, 2011; He and Chen, 2014; Fan et al., 2016). The reason may be that high concentration of H_3O^+ in the solution competes with $Sb(OH)_2^+$ on the active sites of the cell surface when the pH<3.0 (Fan et al., 2008), resulting in a decrease in adsorption efficiency. When the pH reaches 4.0, functional groups, such as carboxyl, hydroxyl and amino groups, with negative charges on the cell surface are exposed to provide more lone pair electrons which combined with

$Sb(OH)_3$ by complexation reaction (Wang et al., 2014), and this process can effectively prevent metals from entering the cell. Therefore, taking both of biomass and biosorption removal rate of Sb(III) into consideration, the suitable pH value of 4 was determined for subsequent experiments in this study.

Temperature not only affects the microbial growth, but also affects accumulation and biosorption for metal ions [42]. As shown in Fig. 1 (f), both the biomass and biosorption removal rate of Sb(III) show an initial increase and then a decrease with increasing temperature (20-40 °C), with a simultaneous maximum values at 28 °C of 7.45 g/L and 58.78%, respectively. The inoculation dose does not have great influences on the biomass, DJHN070401 grows well under inoculation dose of 1-8% with the biomass of 6.86-8.04 g/L (Fig.1(g)). But biosorption removal rate of Sb(III) rises from 13.53% in 1% to 52.73% in 4%, then decreases as the dose continues to increase.

The effect of agitation speed on the biomass and removal of Sb(III) was determined, as shown in Fig. S1(d). It can be concluded that both biomass and removal of Sb(III) by DJHN070401 increases with speed between 90 to 150 r/min. Both biomass and removal of Sb(III) decreased as the speed increased from 150 to 210 r/min. The optimum agitation speed is 150 r/min which consistent with the experimental results of Huang et al. (2013). This can be explained by the increase in agitation speed during biosorption can bring more contact opportunities between the binding sites of microorganism and metal ions, thereby promoting the migration of Sb(III) to the surface of microorganism (Guo et al., 2010; Ucun et al., 2002). But excessive mechanical agitation produces strong shearing forces which causes the vortex formation in the solution (Havelcová et al., 2009), and inhibits cell growth resulting in a decrease in the biosorption of Sb(III).

The effect of initial Sb(III) concentration on biomass and Sb(III) removal rate is shown in Fig. S1 (e). The lower the initial Sb(III) concentration, the adsorption sites on DJHN070401 are relatively abundant and higher adsorption equilibrium and removal results. The metal adsorption sites on the surface of cell wall reached saturation gradually at a high Sb(III) concentration (Deng et al., 2019) . So that the adsorption rate was reduced. In addition, when the initial Sb(III) concentration greater than 50 mg/L, the growth of DJHN070401 was inhibited, but the biomass production remained above 7.0 g/L, indicating that DJHN070401 is highly resistant to Sb(III) (Milová-žiaková et al., 2016).

The biosorption process, as a function of contact time, shows two phases, one fast and one slow, similar to that reported in literature (Wan et al., 2014). The fast adsorption phase is likely to be due to the availability of active sites on adsorbents. When available sorption sites are occupied, adsorption becomes less efficient and leads to a slow adsorption phase. As shown in Fig. 1(h), the adsorption capacity of Sb(III) in the initial 50 min accounts for 81.78%, 64.43%, 53.03% and 72.54% of total adsorption capacities under four initial Sb(III) concentration. The adsorption speed is slow in 420-660 min and almost no change to reach the adsorption equilibrium. It indicates that the biosorption of Sb(III) by DJHN070401 is mainly completed within the first 50 min, as the adsorption continued, Sb(III) is transported to the interior of the cell for accumulation. This implies that the biosorption of Sb(III) by growing microorganisms is caused by cell surface adsorption and internal accumulation (Huang et al., 2013).

Over all, the investigation showed that the eight factors, i.e. carbon source (glucose), pH, temperature, agitation speed, inoculation dose, Fe^{2+}, nitrogen source and $CaCl_2$, have

interdependent influence on biomass yield and Sb(III) removal rate and should further investigated using the Plackett-Burman experiment.

3.2. Plackett-Burman statistical analysis

Plackett-Burman design of eight influencing factors and results on Sb(III) biosorption by DJHN070401 are present in Table 1. Correlation of the environmental parameters to Sb(III) removal rate (Y) by linear regression analysis results in the empirical equations (Eq.3).

$$\begin{aligned} Y = 54.45 + 0.0352X_1 - 3.199X_2 - 0.548X_3 - 0.0152X_4 \\ + 0.323X_5 + 0.0941X_6 + 9.996X_7 + 0.03X_8 \end{aligned} \quad (3)$$

F value is generally used for statistical significance detection, and P value is used to detect the significance of each regression coefficient (Jaafari and Yaghmaeian, 2019). $P<0.0001$ indicates that the model is very significant, while values greater than 0.0500 indicate that the model is not significant under selected conditions, and $0.0001<P<0.05$ indicate that the model is significant (Jaafari and Yaghmaeian, 2019). A determination coefficient (R^2) of 0.9915 of (Eq.3) indicates that only 0.85% cannot be explained by the regression model. Both of R^2 and R_{Adj}^2 (0.9687） are close to 1, indicating that the predicted value is highly consistent with the experimental results. Coefficient of variation of 4.68% is less than 10%, indicating that the model has high reliability and accuracy (Pan et al., 2008). Table S4 analysis shows that pH, Fe^{2+} concentration and temperature have noticeable effects on the Sb(III) removal by DJHN070401 ($P<0.05$), the contribution rate are 48.57%, 42.69% and 5.70%, respectively. However, the influencing factors, such as nitrogen concentration, inoculation dose, glucose concentration, agitation speed and $CaCl_2$, have almost no effects on Sb(III) removal by DJHN070401 ($P>0.05$).

3.3. RSM for optimal biosorption conditions

In order to obtain the best response area for the removal of Sb(III), the central values of levels in the biosorption process are confirmed by a steepest ascent experiment (Table S5) (Bhagwat et al., 2014). The 4th group levels (pH of 4, temperature of 27 ℃ and Fe^{2+} concentration of 1.4 g/L) have the highest removal of 48.83%, at the design center point of the significant factors (Jaafari and Yaghmaeian, 2019).

Through central composite design (CCD) of response surface methodology (RSM), the biosorption conditions of DJHN070401 were optimized. The experimental range of X_1, X_2 and X_6 (maximum and minimum) and levels ($\alpha = 1.68$ (Li et al., 2009)) of independent variables considered as required for the CCD design is presented in Table S6. The complete experiment design matrix and the output responses for Sb(III) biosorption are shown in Table 2. Three replicate runs were used at the center of the design to obtain an estimate of the pure error variance. The quadratic regression models for Sb(III) removal (Y, %) in terms of actual factors as a function of X_1 (Fe^{2+} concentration), X_2 (pH) and X_3 (Temperature) is given as Eq. (4).

$$Y=51.13+0.97X_1-4.25X_2+3.23X_3-0.14X_1X_2+0.44X_1X_3-0.86X_2X_3 -1.27X_1^2-2.11X_2^2-2.64X_3^2 \quad (4)$$

The model equations were evaluated by t-test and the analysis of variance (ANOVA) which revealed that these regressions were statistically significant at 95% confidence level. The values of R^2 for actual and the predicted adsorption efficiency were found to be 0.9643. High R^2 value close to 1, which indicates an adequate agreement between the predicted values obtained from the model and the experimental values. As shown in Table 3, the significance of each coefficient was evaluated by the applying F-value and P-values

(Bhagwat et al., 2014). In this case, the model was highly significant ($P<0.0001$). The lack-of-fit was also calculated from the experimental error (pure error) and residuals. The lack of fit P-value of 0.3274 greater than 0.05 indicating that lack-of-fit for the mathematical models are the insignificant and the quadratic model was valid and significance of the model correlation between the variable and process response for the biosorption of Sb(III) using DJHN070401 (Pan et al., 2008).

The interaction effects between observed variables Fe^{2+} concentration, pH and temperature on biosorption removal rate of Sb(III) are shown in Fig. 2. The removal rate is directly proportional to temperature (Fig. 2(a)), and is inversely proportional to pH (Fig. 2(c)). With Fe^{2+} concentration enrichment, the removal rate increased first (1.2-1.5g/L) and then decreased slightly (1.5-1.6g/L). Moreover, contour plots in Fig.2(b,d) is almost circular, indicating that interaction effects between temperature and pH, Fe^{2+} concentration and pH are not significant (Bhattacharjee and Joshi, 2016; Tomas et al., 2004). Meanwhile, contour plots in Fig. 2(f) is elliptical, indicating that interaction effects between temperature and Fe^{2+} concentration is significant. Therefore, appropriately increasing Fe^{2+} concentration and temperature, and reducing the pH can enhance biosorption removal rate of Sb(III) by DJHN070401. The total adsorption sites in DJHN070401 cells increased with Fe^{2+} enrichment and is favorable for adsorption (Iqbal et al., 2013), but the biomass yield and iron enrichment ability of DJHN070401 decreases with the increase of Fe^{2+} in the medium and is unfavorable for adsorption (Iqbal et al., 2013; Lopičic´ et al., 2013). As highlighted in section 3.1, the most suitable pH for Sb(III) biosorption is between.3.0 and 4.0 (Urík et al., 2019). The effect of temperature on biosorption generally expressed as diffusion coefficients of adsorbates increase with

increasing temperature, enhancing Sb(III) diffusion in adsorbent channels improving the removal efficiency.

The main purpose of the experimental studies was to obtain the optimal values of variables for Sb(III) removal using DJHN070401. The theoretical optimal biosorption conditions for removal Sb(III) was calculated from the Eq.(4), for which Fe^2 concentration of 1.51 g/L, pH=3.50, and temperature of 28.60 ℃, and the maximum predicted value (Y_{pre}) of Sb(III) removal rate was 55.2% in this study. A series of three sets of experiments were repeated under optimal conditions to determine the maximum Sb(III) removal experimentally, the average removal of Sb(III) was found to be 56.83%, only 1.63% difference between the predicted and the observed values. The capacity for and removal of Sb(III) by DJHN070401 was compared with other microorganisms reported in the literature and listed in Table 4. If only the effect of biosorption is considered, DJHN070401 show comparable with and higher ability than many living microorganisms reported in the literature, such as *Sphaerotilus natans* (Li et al., 2018), sulfate-reducing bacteria (Zhang et al., 2016), aerobic granules (Wang et al., 2014), fungi aerobic granules (Wan et al., 2014). The results indicate that the optimization method based on RSM is feasible and Sb(III) removal was greatly improved.

3.4. Identifying the mechanism of Sb(III) Biosorption

SEM-EDS characterization of DJHN070401 before and after Sb(III) biosorption are shown in the Fig.S2. The surface morphology of DJHN070401 before Sb(III) was uneven and the blocky texture provides a multi-site adsorption surface for the Sb(III) biosorption (Fig.S2(a)). Moreover, large contact area for adsorbing Sb(III) created due to the presence of various gaps, pores, void structures. After biosorption (Fig. S2(b)), the surface

morphology of DJHN070401 was changed, which was mainly reflected in the obvious reduction of voids and blurring of surface edges. The main elements of DJHN070401 were O (29.85%) and C (34.48%), which provides a possibility for the complexation of Sb(III) by groups. As shown in Fig. S2(b), it can be seen that the absorption peak of antimony appears near the binding energy of 3.0-3.5 KeV after adsorption. Moreover, the sorbed mass of antimony increases to 1.58% after biosorption, indicating that Sb(III) is complexed with functional groups on the surface of cell wall (Iqbal et al., 2013; Sun et al., 2011). The decrease in Na, Ca and Fe indicated ion exchange reactions take place during the biosorption process (Deng et al., 2018; Iqbal et al., 2013). It is speculated that the addition of Ca^{2+} and Fe(II) forms a ternary complex $Fe(OH)_3$-Ca-Sb (Guan et al., 2009), was also tentatively verified by XRD (Fig.4), which may promote Sb(III) biosorption.

Because extracellular adsorption was the dominating Sb(III) adsorptive mode, FTIR analysis was used to identify functional groups for biosorption and postulate the mechanism by reviewing the functional groups identified and their displacement, as shown in Fig.3. Characteristic absorption peaks were identified at 3394, 1711, 1540, 1409, 1031 cm^{-1}, respectively. After biosorption, these absorption peaks shifted to 3398, 1745, 1560, 1383, and 1045 cm^{-1}, respectively. Among them, the peak of 3394 cm^{-1} shifted 4 cm^{-1} indicated that the amino group (-NH) and the hydroxyl group (-OH) in the polysaccharide, fatty acid and protein reacted with Sb(III) (Wu et al., 2012; Iqbal et al., 2013; Sun et al., 2011). But this reaction had little effect on Sb(III) biosorption by DJHN070401. A strong absorption peak at 2924 cm^{-1}, which was assigned to the C=H bonds of aliphatic acids, symmetric or asymmetric (Ma et al., 2011; Wu et al., 2012), was not obvious change before and after biosorption. The peak at 1711 cm^{-1} may cause by the

stretching vibration of the C=O bond in carboxylic acid, and shifted 34 cm^{-1} indicates that the carboxylic acid group on the cell wall surface chemically reacts with Sb(III) (Huang et al., 2013; Wan et al., 2014). The -NH bending vibration in amide-II band was shown by the peak at 1540 cm^{-1} (Sun et al., 2011; Wu et al., 2012), and it was shown by the peak at 1560 cm^{-1} after biosorption which indicated the amino group in the protein participated in biosorption. The peak at 1409 cm^{-1} represents symmetrical stretching of-COOH (Anand et al., 2006; Wu et al., 2012), and moved to 1383 cm^{-1} indicates that carboxyl group provided a biosorption site on the cell wall surface. Besides, the effects of pH values on the biosorption largely depend on the speciation of Sb and protonation of functional groups on the cell surface of the biosorbent. At pH 4, the carboxyl group could be protonated and exists in the molecular state (-COOH), and surface complexed with neutral $Sb(OH)_3$ via Sb-O-C bond to establish a linear or five cyclic bidendate complexes (Tella et al., 2008), $Sb(OH)_3$ also undergoes hydrogen bonding with carboxyl or hydroxyl groups (Wu et al., 2012). The peak at 1031 cm^{-1}, which represents the stretching vibration of the C-O group of cell wall polysaccharides, shifted significantly to 1045 cm^{-1}, indicating that the polysaccharide molecules may complex with Sb(III) during the biosorption (Xu et al., 2015). A new peak at 1153 cm^{-1}, mainly causing by symmetric and asymmetric stretching vibration of PO^{2-} and $P(OH)_2$ on the phosphate group after Sb(III) biosorption (Choudhary et al., 2009), implied that the phosphate group was complexed with Sb(III). Moreover, the bending vibration absorption peak at 607 cm^{-1} disappeared after biosorption, hinting that the phosphate group (PO_4^{3-}) has completely reacted (Pradhan et al., 2007). Changes of protein peaks (1653, 1242 cm^{-1}) is not distinct after biosorption (Lin et al., 2012; Huang et al., 2013), indicating that the main components and structure of DJHN070401 are still intact after biosorption of

Sb(III). Overall, these results indicated that the chemical interactions of ion exchange between the metal ions and the hydrogen atoms of carboxylic acid group, hydroxyl, amino groups of the biomass engage in the biosorption process.

Due to the complex composition of DJHN070401 thallus, biosorption occurs when contacting with the Sb-containing liquids and produces compounds as XRD spectrum shows (Fig. 4). $Ca_2Fe(SbO_6)$, $Ca_{11}Sb_{10}$, $FeSb_2O_6$ and $FeSbO_4$ have strong diffraction peaks, indicating that the chemical interaction happened between $CaCl_2$, Sb(III) and Fe(Ⅱ) enriched in the yeast. It is concluded that Ca^{2+} is beneficial to promote Sb(III) biosorption and verified with Fig. S1 (c), which was consistent with Miao et al. (2014). Ca(II) induced adsorption enhancement of antimony possibly resulted from the formation of HFO-Ca-Sb complexes (Miao et al., 2014) or form secondary minerals with Ca^{2+}, Mg^{2+}, K^+, etc. (Okkenhaug et al., 2012), which precipitates on the cell surface. Guan et al. (2009) revealed that the improvement of As(III) removal in the $KMnO_4$-Fe(II) process by Ca^{2+} was associated with the formation of monodentate complex of $Fe(OH)_3$-Ca-As and Ca^{2+} increased the surface charge.

3.5. Effect of DCC inhibitor on Sb(III) biosorption efficiency

Metabolic inhibitors, such as DCC, can greatly inhibit the growth of the microbes and may reduce the continuous metabolic metals uptake of the living cells which may be used for bioremediation (Luo et al., 2011). The Sb(III) biosorption removal rates were analyzed and compared in culture medium with or without DCC (Fig. 5). It is noticed that the biosorption of Sb(III) by DJHN070401 can be divided into two stages. In the adaptation period (0-6 h), the Sb(III) biosorption rates of without and with DCC were 31.13% and

27.22%, respectively. The possible reason was that DCC inhibited the microbial growth, so that the extracellular binding site in the cell wall was reduced (Guo et al., 2010), which resulted in induced biosorption rates. These results also indicated that there was biological adsorption independent of energy metabolism during adaptation period (Luo et al., 2011). In the logarithmic growth phase, the Sb(III) biosorption rates of with DCC was about 5% higher than that of without DCC. It implied that DCC can improve the Sb(III) biosorption rates in the later growth stage, and there was bioaccumulation based on energy metabolism during the logarithmic growth phase. Some studies had indicated that DCC did not damage the cell wall structure of microorganisms (Huang et al., 2014; Luo et al., 2011), but inhibited the ion efflux process of microorganisms (Anand et al., 2006; Xiao et al., 2010). As a result, as more and more Sb(III) ions accumulate in the interior of the cells, which resulted in increasing biosorption. In conclusion, cell wall adsorption (biosorption independent of energy metabolism) plays a leading role in the Sb(III) biosorption process of DJHN070401. To the best of our knowledge, few reported microbe (Luo et al., 2011; Huang et al., 2013), whose metal bioremediation efficiency did not decrease like any other reported strains (Anand et al., 2006; Radhika et al., 2006; Malekzadeh et al., 2002) but increase in the presence of metabolic inhibitors. Therefore, DJHN070401 may be a potential resource of highly efficient candidates for heavy metal bioremediation due to their unique characteristics which were obtained in their original special inhibition niches of hyperaccumulator.

4. Conclusion

We report on the method and approach to enhance biosorption of Sb(III) onto living *Rhodotorula mucilaginosa* strain DJHN070401 using RSM with CCD statistical analysis. The influence of the nutritional and environmental factors such as the Fe^{2+} concentration, pH and temperature were considered. The results revealed that the CCD design could be successfully applied for the modeling and optimizing the process variables and interactions in the response. Additionally appropriate calcium and ferrous ion concentrations are beneficial for Sb(III) biosorption onto strain DJHN070401. Surface complexation and ion exchange are main mechanism for biosorption. DJHN070401 is a suitable, candidate for antimony removal in industrial effluents where it is robust against increasing loading of metabolic inhibitors.

Acknowledgments

This study was financially supported by the National Natural Science Foundation of China (No. 41672350, 51604113) and the scientific research project of the Hunan Provincial Education Department (No.18A184). Andrew S. Hursthouse acknowledges the support of Hunan Provincial Government and Hunan University of Science & Technology through the High End Expert Scholarship.

References

1. Anand, P., Isar, J., Saran, S., Saxena, K.R., 2006. Bioaccumulation of copper by *Trichoderma viride*. **Bioresource Technology** 97(8), 1018-1025.

2. Banerjee, A., Sarkar, P., Banerjee, S., 2016. Application of statistical design of experiments for optimization of As(V) biosorption by immobilized bacterial biomass. Ecological Engineering 86, 13-23.
3. Bhagwat, P.K., Jhample, S.B., Dandge, P.B., 2015. Statistical medium optimization for the production of collagenolytic protease by *Pseudomonas* sp. SUK using response surface methodology. Microbiology 84(4), 520-530.
4. Bhattacharjee, K., Joshi, S.R., 2016. A selective medium for recovery and enumeration of endolithic bacteria. Journal of Microbiological Methods 129, 44-54.
5. Bhosale, P., Gadre, R.V., 2001. Production of β-carotene by a *Rhodotorula glutinis* mutant in sea water medium. **Bioresource Technology** 76(1), 53-55.
6. Choudhary, S., Sar, P., Characterization of a metal resistant *Pseudomonas* sp. isolated from uranium mine for its potential in heavy metal (Ni^{2+}, Co^{2+}, Cu^{2+}, and Cd^{2+}) sequestration. **Bioresource Technology** 100(9), 2482-2492.
7. Deng, R.J., Jin, C.S., Ren, B.Z., Hou, B.L., Hursthouse, A.S., 2017. The potential for the treatment of antimony-containing wastewater by Iron-based adsorbents. Water 9(10), 794.
8. Deng, R.J., Jin, C.S., Hou, B.L., Tang, Z.E., Ren, B.Z., 2018. Research progress of microorganism treating antimony containing wastewater. Environmental Pollution & Control 40(4), 465-472. (*in Chinese*)
9. Deng, R.J., Shao, R., Ren, B.Z., Hou, B.L., Tang, Z.E., Hursthouse, A.S., 2019. Adsorption of antimony(III) onto Fe(III)-treated humus sludge adsorbent: Behavior and mechanism insights. Polish Journal of Environmental Studies 28(2), 577-586.
10. Fan, H.T., Sun, W., Jiang, B., Wang, Q.J., Li, D.W., Huang, C.C., Wang, K.J., Zhang, Z.G., 2016. Adsorption of antimony(III) from aqueous solution by mercapto-

functionalized silica-supported organic-inorganic hybrid sorbent: Mechanism insights. Chemical Engineering Journal 286, 128-138.

11. Fan, T., Liu, Y.G., Feng, B.Y., Zeng, G.M., Yang, C.P., Zhou, M., Tan, Z.F., Wang, X., 2008. Biosorption of cadmium(II), zinc(II) and lead(II) by *Penicillium simplicissimum*: Isotherms, kinetics and thermodynamics. Journal of Hazardous Materials 160(2), 655-661.
12. Guo, H.J., Luo, S.L., Chen, L., Xiao, X., Xi, Q., Wei, W.Z., Zeng, G.M., Liu C.B., Wan, Y., Chen, J.L., He, Y.J., 2010. Bioremediation of heavy metals by growing hyperaccumulaor endophytic bacterium *Bacillus* sp. L14. **Bioresource Technology** 101(2), 8599-8605.
13. Guan, X.H., Ma, J., Dong, H.R., Jiang, L., 2009. Removal of arsenic from water: effects of competing anions on As(III) removal in KMnO4-Fe(II) process. Water Research. 43(15), 3891-3899.
14. Guo, X.J., Wu, Z.J., He, M.C., Meng, X.G., Jin, X., Qiu, N., Zhang, J., 2014. Adsorption of antimony onto iron oxyhydroxides: Adsorption behavior and surface. Journal of Hazardous Materials 276(9), 339-345.
15. Havelcová, M., Mizera, J., Sýkorová, I., Pekař, M., 2009. Sorption of metal ions on lignite and the derived humic substances. Journal of Hazardous Materials. 161(1), 559-564.
16. He, J.S., Chen, J.P., 2014. A comprehensive review on biosorption of heavy metals by algal biomass: Materials, performances, chemistry, and modeling simulation tools. **Bioresource Technology** 160(6), 67-78.
17. He, M.C., Wang, X.Q., Wu, F.C., Fu, Z.H., 2012. Antimony pollution in China. Science of the Total Environment 421-422(3), 41-50.

18. He, M.C., Wang, N.N., Long, X.J., Zhang, C.J., Ma, C.L., Zhong, Q.J., Wang, A.H., Wang, Y., Pervaiz, A., Shan, J., 2019. Antimony speciation in the environment: Recent advances in understanding the biogeochemical processes and ecological effects. Journal of Environmental Sciences 75, 14-39.
19. Henckens, M.L.C.M., Driessen, P.P.J., Worrell, E., 2016. How can we adapt to geological scarcity of antimony? Investigation of antimony's substitutability and of other measures to achieve a sustainable use. Resources Conservation & Recycling 108, 54-62.
20. Herath, I., Vithanage, M., Bundschuh, J., 2017. Antimony as a global dilemma: Geochemistry, mobility, fate and transport. Environmental Pollution 223, 545-549.
21. Huang, F., Dang, Z., Guo, C.L., Lu, G.N., Gu R.R., Liu, H.J., Zhang, H., 2013. Biosorption of Cd(II) by live and dead cells of *Bacillus cereus* RC-1 isolated from cadmium-contaminated soil. Colloids and Surfaces B: Biointerfaces 107, 11-18.
22. Huang, F., Guo, C.L., Lu, G.N., Yi, X.Y., Zhu, L.D., Dang, Z., 2014. Bioaccumulation characterization of cadmium by growing *Bacillus cereus* RC-1 and its mechanism. Chemosphere 109, 134-142.
23. Iqbal, M., Saeed, A., Edyvean, R.G.J., 2013. Bioremoval of antimony(III) from contaminated water using several plant wastes: Optimization of batch and dynamic flow conditions for sorption by green bean husk (V*igna radiata*). Chemical Engineering Journal 225(3), 192-201.
24. Jaafari, J., Yaghmaeian, K., 2019. Optimization of heavy metal biosorption onto freshwater algae (*Chlorella coloniales*) using response surface methodology (RSM). Chemosphere 217, 447-455.

25. Li, J., Wang, Q., Zhang, S.Z., Qin, D., Wang, G.J., 2013. Phylogenetic and genome analyses of antimony-oxidizing bacteria isolated from antimony mined soil. International Biodeterioration & Biodegradation 76, 76-80.
26. Li, J.Y., Zheng, B.H., He, Y.Z., Zhou, Y.Y., Chen, X., Ruan, S., Yang, Y., Dai, C.H., Tang, L., 2018. Antimony contamination, consequences and removal techniques: A review. Ecotoxicology & Environmental Safety 156, 125-134.
27. Li, M.S., Li, J., Wang, G.J., 2013. Research advances in microbial mechanism of antimony. Journal of Huazhong Agricultural University 45(5), 15-19. (*in Chinese*)
28. Li, X.D., Jia, R., Li, P.S., Ang, S.S., 2009. Response surface analysis for enzymatic decolorization of Congo red by manganese peroxidase. Journal of Molecular Catalysis B：Enzymatic 56(1), 1-6.
29. Li, X.J., Cheng, Y.X., Gong, D.X., Xiang, R.J., 2012. *Bacillus* sp. treating wastewater containing antimony. Environmental Science & Technology 35(2), 162-166. (*in Chinese*)
30. Li, Y.C., Wu, J.X., Hu, W., Ren, B.Z., Hursthouse, A.S., 2018. A mechanistic analysis of the influence of iron-oxidizing bacteria on antimony(V) removal from water by microscale zero valent iron. Journal of Chemical Technology & Biotechnology 93, 2527-2534.
31. Lialikova, N.N., 1974. Stibiobacter senarmontii-a new microorganism oxidizing antimony. Mikrobiologiya 43(6), 941-948.
32. Lin, Y.B., Wang, X.Y., Wang, B.P., Mohamad, O., Wei, G.H., 2012. Bioaccumulation characterization of zinc and cadmium by *Streptomyces zinciresistens*, a novel actinomycete. Ecotoxicology & Environmental Safety 77, 7-17.

33. Lopičic´, Z.R., Milojkovic´, J.V., Šoštaric´, T.D., Petrović, M.S., Mihajlović, M.L., Lačnjevac, C.M., Stojanović, M.D., 2013. Influence of pH value on Cu(II) biosorption by lignocellulose peach shell waste material. Hemijska Industrija 67(6), 1007-1015.

34. Luo, S.L., Xiao, X., Xi, Q., Wan, Y., Chen, L., Zeng, G.M., Liu, C.B., Guo, H.J., Chen, J.L., 2011. Enhancement of cadmium bioremediation by endophytic bacterium *Bacillus* sp. L14 using industrially used metabolic inhibitors (DCC or DNP). Journal of Hazardous Materials 190(1-3), 1079-1082.

35. Ma, Y., Lin, J.Q., Zhang, C.J., Ren, Y.L., Lin, J.Q., 2011. Cd(II) and As(III) bioaccumulation by recombinant *Escherichia oli* expressing oligomeric human metallothioneins. Journal of Hazardous Materials 185(2-3), 1605-1608.

36. Macgregor, K., Mackinnon, G., Farmer, J.G., Graham, M.C., 2015. Mobility of antimony, arsenic and lead at a former antimony mine, Glendinning, Scotland. Science of The Total Environment 529, 213-222.

37. Malekzadeh, F., Latifi, A.M., Shahamat, M., Levin, M., Colwell, R.R., 2002. Effects of selected physical and chemical parameters on uranium uptake by the bacterium *Chryseomonas* MGF-48. World Journal of Microbiology and Biotechnology 18(7), 599-602.

38. Miao, Y.Y., Han, F.C., Pan, B.C., Nie, G.Z., Lv, L., 2014. Antimony(V) removal from water by hydrated ferric oxides supported by calcite sand and polymeric anion exchanger. Journal of Environmental Sciences 26(2), 307-314.

39. Milová-žiaková, B., Urík, M., Boriová, K., Bujdoš, M., Kolenčík, M., Mikušová, P., Takáčová, A., Matúš, P., 2016. Fungal solubilization of manganese oxide and its

significance for antimony mobility. International Biodeterioration & Biodegradation 114, 157-163.

40. Mittal, V.K., Bera, S., Narasimhan, S.V, Velmurugan, N.S., 2013. Adsorption behavior of antimony(III) oxyanions on magnetite surface in aqueous acid environment. Applied Surface Science 266(2), 272-279.
41. Nguyen, V.K., Choi, W.Y., Yu, J., Lee, T., 2017. Microbial oxidation of antimonite and arsenite by bacteria isolated from antimony-contaminated soils. International Journal of Hydrogen Energy 42(45), 27832-27842.
42. Okkenhaug, G., Zhu, Y.G., He, J.W., Li, X., Luo, L., Mulder, J., 2012. Antimony (Sb) and Arsenic (As) in Sb mining impacted paddy soil from Xikuangshan, China: Differences in mechanisms controlling soil sequestration and uptake in rice. Environmental Science & Technology 46(6), 3155-3162.
43. Uluozlu, O.D., Sarı, A., Tuzen, M., 2010. Biosorption of antimony from aqueous solution by lichen (*Physcia tribacia*). Chemical Engineering Journal 163(3), 382-388.
44. Urík, M., Polák, F., Bujdoš, M., Miglierini, M., Milová-Žiaková, B., Bence, F., Goneková, Z., Vojtková, H., Matúš, P., 2019. Antimony leaching from antimony-bearing ferric oxyhydroxides by filamentous fungi and biotransformation of ferric substrate. Science of The Total Environment 664, 683-689.
45. Pan, C.M., Fan, Y.T., Xing, Y., Hou, H.W., Zhang, M.L., 2008. Statistical optimization of process parameters on biohydrogen production from glucose by *Clostridium* sp. Fanp2. **Bioresource Technology** 99(8), 3146-3154.

46. Pradhan, S., Singh, S., Rai, L.C., 2007. Characterization of various functional groups present in the capsule of *Microcystis* and study of their role in biosorption of Fe, Ni and Cr. **Bioresource Technology** 98(3), 595-601.

47. Radhika, V., Subramanian, S., Natarajan, K.A., 2006. Bioremediation of zinc using *Desulfotomaculum nigrificans*: bioprecipitation and characterization studies. Water Research 40(19), 3628-3636.

48. Reddy, L.V.A., Wee, Y.J., Yun, J.S., Ryu. H.W., 2008. Optimization of alkaline protease production by batch culture of *Bacillus* sp. RKY3 through Plackett-Burman and response surface methodological approaches. **Bioresource Technology**. 99(7), 2242-2249.

49. Shin, Y.M., Kwon, T.H., Kim, K.S., Chae, K.S., Kim, D., Kim, J.H.O., Yang, M.S., 2001. Enhanced iron uptake of *Saccharomyces cerevisiae* by heterologous expression of a tadpole ferritin gene. Applied & Environmental Microbiology 67(3), 1280-1283.

50. Sun, F.H., Wu, F.C., Liao, H.Q., Xing, B.S., 2011. Biosorption of antimony(V) by freshwater cyanobacteria Microcystis biomass: chemical modification and biosorption mechanisms. Chemical Engineering Journal 171(3), 1082-1090.

51. Sun, W.M., Xiao, E.Z., Kalin, M., Krumins, V., Dong, Y.R., Ning, Z.P., Liu, T., Sun, M., Zhao, Y.L., Wu, S.L., Mao, J.Z., Xiao, T.F., 2016. Remediation of antimony-rich mine waters: Assessment of antimony removal and shifts in the microbial community of an onsite field-scale bioreactor. Environmental Pollution 215(2), 213-222.

52. Tella, M., Pokrovski, G.S., 2008. Antimony(V) complexing with O-bearing organic ligands in aqueous solution: An X-ray absorption fine structure spectroscopy and potentiometric study. Mineralogical Magazine 72(1), 205-209.

53. Tomas, V.S., Zetić, V.G., Stanzer, D., Grba, S., Vahčić, N., 2004. Zinc, Copper and Manganese Enrichment in Yeast *Saccharomyces cerevisae*. Food Technology & Biotechnology 42(2), 115-120.

54. Ucun, H., Bayhan, Y.K., Kaya, Y., Cakici, A., Algur, O.F., 2002. Biosorption of chromium(VI) from aqueous solution by cone biomass of *Pinus sylvestris*. **Bioresource Technology** 85(2), 155-158.

55. Ungureanu G, Santos S, Boaventura R, Botelho, C., 2015. Arsenic and antimony in water and wastewater: Overview of removal techniques with special reference to latest advances in adsorption. Journal of Environmental Management. 151, 326-342.

56. Vijayaraghavan, K., Balasubramanian, R., 2011. Antimonite removal using marine algal species. Industrial and Engineering Chemistry Research 50(17), 9864-9869.

57. Wan, C.L., Wang, L., Lee, D.J., Zhang, Q.L., Li, J.N., Liu, X., 2014. Fungi aerobic granules and use of Fe(III)-treated granules for biosorption of antimony(V). Journal of the Taiwan Institute of Chemical Engineers. 45(5), 2610-2614.

58. Wang, H.W., Chen, F.L., Mu, S.Y., Zhang, D.Y., Pan, X.L., Lee, D.J., Chang, J.S., 2013. Removal of antimony(Sb(V)) from Sb mine drainage: Biological sulfate reduction and sulfide oxidation-precipitation. **Bioresource Technology**. 146(10), 799-802.

59. Wang, L., Wan, C.L., Lee, D.J., Liu, X., Zhang, Y., Chen, X.F., Tay, J.H., 2014. Biosorption of antimony(V) onto Fe(III)-treated aerobic granules. **Bioresource Technology** 158(2), 351-354.

60. Wang, N.N., Wang A.H., Xie, J., He, M.C., 2019. Responses of soil fungal and archaeal communities to environmental factors in an ongoing antimony mine area. Science of The Total Environment 652, 1030-1039.

61. Wu, F.C., Sun, F.H., Wu, S., Yan, Y.B., Xing, B.S., 2012. Removal of antimony(III) from aqueous solution by freshwater cyanobacteria *Microcystis* biomass. Chemical Engineering Journal 183(4), 172-179.

62. Xi, J.H., He, M.C., Lin, C.Y., 2011. Adsorption of antimony(III) and antimony(V) on bentonite: kinetics, thermodynamics and anion competition. Microchemical Journal 97(1), 85-91.

63. Xiao, X., Luo, S.L., Zeng, G.M., Wei, W.Z., Wan, Y., Chen, L., Guo, H.J., Yang, L.X., Chen, J.L., Xi, Q., 2010. Biosorption of cadmium by endophytic fungus (EF) *Microsphaeropsis* sp. LSE10 isolated from cadmium hyperaccumulator *Solanum nigrum* L. **Bioresource Technology** 101(6):1668-1674.

64. Xu, W., Wang H.J., Liu, R.P., Zhao, X., Qu, J.H., 2011. The mechanism of antimony(III) removal and its reactions on the surfaces of Fe-Mn binary oxide. Joumal of colloid and interface science 363(1), 320-326.

65. Xu, W.H., Jian, H., Liu, Y.G., Zeng, G.M., Li, X., Gu, Y.L., Tan, X.F., 2015. Removal of Chromium (VI) from Aqueous Solution Using Mycelial Pellets of *Penicillium simplicissimum* Impregnated with Powdered Biochar. Bioremediation Journal 19(4), 259-268.

66. Zaki, S., Abd-EI-Haleem, D., Abulhamd, A., Elbery, H., AbuElreesh G., 2008. Influence of phenolics on the sensitivity of free and immobilized bioluminescent Acinetobacter bacterium. Microbiological Research 163(3), 277-285.

67. Zhang, D.Y., Pan, X.L., Zhao, L., Mu, G.J., 2011. Biosorption of Antimony (Sb) by the Cyanobacterium *Synechocystis* sp. Polish Journal of Environmental Studies 20(5), 1353-1358.

68. Zhang, G.P., Ouyang, X.X., Li, H.X., Fu, Z.P., Chen, J.J., 2016. Bioremoval of antimony from contaminated waters by a mixed batch culture of sulfate-reducing bacteria. International Biodeterioration and Biodegradation 115(12), 148-155.

Table 1: Placket-Burman design and results

Run	Variables and levels								Y/(%)	
no.	X_1	X_2	X_3	X_4	X_5	X_6	X_7	X_8	Y_{exp}	Y_{pre}
1	+1	+1	+1	-1	-1	+1	-1	+1	20.13	18.53
2	+1	+1	-1	-1	+1	+1	+1	-1	23.83	24.28
3	-1	-1	+1	-1	+1	+1	+1	-1	48.82	48.37
4	-1	+1	+1	+1	+1	-1	-1	-1	25.53	23.72
5	+1	-1	-1	-1	+1	-1	-1	+1	11.19	10.54
6	+1	+1	-1	+1	-1	-1	+1	-1	7.24	6.79
7	-1	+1	-1	+1	+1	+1	-1	+1	41.61	43.42
8	+1	-1	+1	+1	-1	+1	-1	-1	25.72	27.33
9	-1	-1	-1	+1	-1	+1	+1	+1	52.39	50.58
10	+1	-1	+1	+1	+1	-1	+1	+1	12.83	13.48
11	-1	-1	-1	-1	-1	-1	-1	-1	27.29	27.94
12	-1	+1	+1	-1	-1	-1	+1	+1	20.47	22.07

Table 2: experimental factors in coded units and experimental responses

Run no.	Codes values			Sb(III) removal (%)		Run no.	Codes values			Sb(III) removal (%)	
	X_1	X_2	X_3	Y_{exp}	Y_{pre}		X_1	X_2	X_3	Y_{exp}	Y_{pre}
1	1	-1	-1	45.44	45.94	11	0	0	0	49.15	51.13
2	0	0	0	52.25	51.13	12	-1	-1	-1	44.33	44.6
3	-α	0	0	45.18	45.92	13	0	0	-α	39.25	38.25
4	1	1	-1	38.72	38.88	14	0	0	0	50.57	51.13
5	0	0	0	50.7	51.13	15	0	0	0	51.6	51.13
6	0	+α	0	37.14	38.03	16	0	-α	0	51.98	52.31
7	0	0	+α	46.88	49.11	17	-1	1	1	43.28	41.96
8	+α	0	0	48.72	49.18	18	1	-1	1	55.98	55
9	1	1	1	45.57	44.5	19	0	0	0	52.7	51.13
10	-1	1	-1	37.95	38.1	20	-1	-1	1	52.88	51.9

Table 3: ANOVA analysis for variance of the model

Source of variations	Mean square	Degrees of freedom	Sun of squares	F	P
Model	570.64	9	63.40	30.04	<0.0001
X_1	12.80	1	12.80	6.07	0.0335
X_2	246.94	1	246.94	117.01	<0.0001
X_3	142.40	1	142.40	67.48	<0.0001
X_1X_2	0.17	1	0.17	0.079	0.7840
X_1X_3	1.55	1	1.55	0.73	0.4115
X_2X_3	5.98	1	5.98	2.83	0.0131
X_1^2	23.16	1	23.16	10.97	0.0078
X_2^2	64.38	1	64.38	30.51	0.0003
X_3^2	100.61	1	100.61	47.67	<0.0001
Residual error	21.10	10	2.11		
Lack of fit	12.74	5	2.55	1.52	0.3274
Pure error	8.36	5	1.67		
Total error	591.75	19			
R^2	0.9643				
R_{Adj}^2	0.9322				

Table 4: comparison of biosorption capacities of various microorganism for antimony

Microorganism	Initial con-centration (mg/L)	Sb oxidation state	pH	Temperature (K)	Adsorbent dose (g/L)	Contact time (h)	Dead or living bacteria	Removal Rate (%)	Reference
Sphaerotilus natans	40	Sb(V)	7	30	2%	72	living	5.4*	[9]
Bacillus sp.	120	Sb(V)	2	30	5%	96	living	99.75**	[16]
Sulfate-reducing bacteria							living		[15]
Sulfate-reducing bacteria	5	Sb(V)	7.2	30	-	96	living	32*	[12]
Turbinaria conoides	5	Sb(III)	7.2	30	0.2-0.8	96	living	13*	[17]
Aerobic granules	20	Sb(V)	2.0	35	-	3	living	21*	[14]
Fungi aerobic granules	20	Sb(V)	3.4	35	-	-	living	23.2*	[15]
Freshwater Cyanobacteria	10	Sb(V)	2.5	25	50	2	dead	32*	[53]
Microcystis biomass	10	Sb(III)	4.0	25	50	1	dead	85**	[18]
Physcia tribacia	10	Sb(III)	3.0	20	4.0	0.5	dead	96**	[27]
Turbinaria conoides	100	Sb(III)	6.0	23	2.0	0.75	dead	95**	[17]
Sargassum sp.	100	Sb(III)	6.0	23	2.0	0.75	dead	72.1**	[17,19]
DJHN070401	20	Sb(III)	3.5	28.6	0.5%	24	living	56.8*	This study

Fig. 1: Effect of nutritional factors ((a) carbon source, (b) nitrogen source, (c) $CaCl_2$ concentration, (d) Fe^{2+} concentration) and environmental factors ((e) initial pH, (f) temperature, (g) inoculation dose, (h) time) on biomass and Sb(III) biosorption of living *Rhodotorula mucilaginosa* DJHN070401.

Fig. 2: 3D response surfaces (a) and 2D contour line (b) for Sb(III) removal rate as function of pH and Fe^{2+} concentration; 3D response surfaces (c) and 2D contour line (d) for Sb(III) removal rate as function of temperature and pH; 3D response surfaces (e) and 2D contour line (f) for Sb(III) removal rate as function of temperature and Fe^{2+} concentration.

Fig. 3: FTIR spectrum of *Rhodotorula mucilaginosa* DJHN070401 before and after Sb(III) biosorption.

Fig. 4: XRD analysis for *Rhodotorula mucilaginosa* DJHN070401 after Sb(III) biosorption.

Fig. 5: Effect of metabolic inhibitor (DCC) on Sb(III) biosorption. (0-6h: adaptation period; 12-18h: logarithmic growth phase; 18-30h: stable growth phase.)

Fig. 1

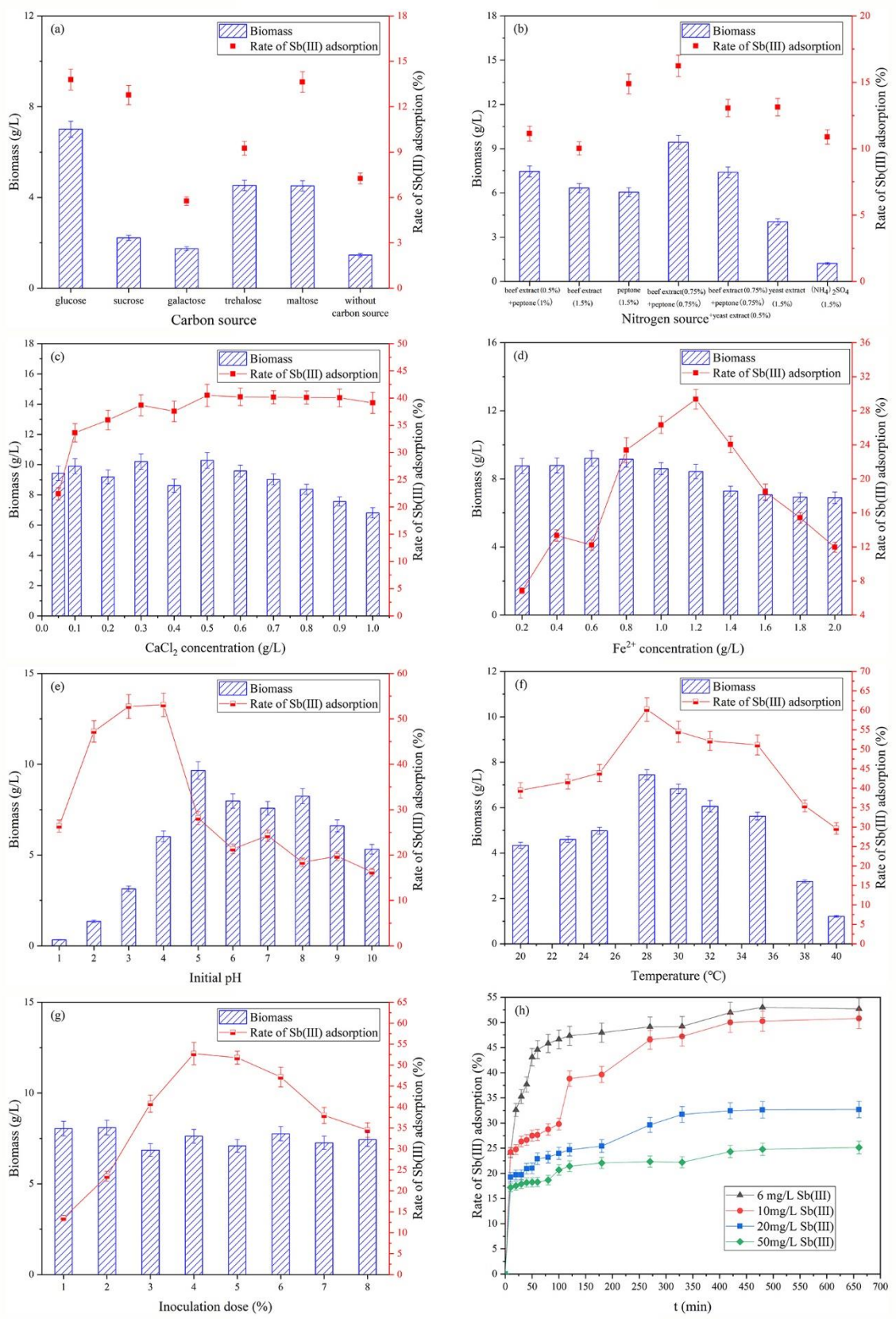
(a)
Biomass
Rate of Sb(III) adsorption
Biomass (g/L)
Rate of Sb(III) adsorption (%)
glucose
sucrose
galactose
trehalose
maltose
without carbon source
Carbon source
(b)
Biomass
Rate of Sb(III) adsorption
Biomass (g/L)
Rate of Sb(III) adsorption (%)
beef extract (0.5%) +peptone (1%)
beef extract (1.5%)
peptone (1.5%)
beef extract(0.75%) +peptone (0.75%)
beef extract (0.75%) +peptone (0.75%)
yeast extract (1.5%)
(NH4)2SO4 (1.5%)
Nitrogen source +yeast extract (0.5%)
(c)
Biomass
Rate of Sb(III) adsorption
Biomass (g/L)
Rate of Sb(III) adsorption (%)
CaCl2 concentration (g/L)
(d)
Biomass
Rate of Sb(III) adsorption
Biomass (g/L)
Rate of Sb(III) adsorption (%)
Fe2+ concentration (g/L)
(e)
Biomass
Rate of Sb(III) adsorption
Biomass (g/L)
Rate of Sb(III) adsorption (%)
Initial pH
(f)
Biomass
Rate of Sb(III) adsorption
Biomass (g/L)
Rate of Sb(III) adsorption (%)
Temperature (℃)
(g)
Biomass
Rate of Sb(III) adsorption
Biomass (g/L)
Rate of Sb(III) adsorption (%)
Inoculation dose (%)
(h)
Rate of Sb(III) adsorption (%)
6 mg/L Sb(III)
10mg/L Sb(III)
20mg/L Sb(III)
50mg/L Sb(III)
t (min)

Fig. 2

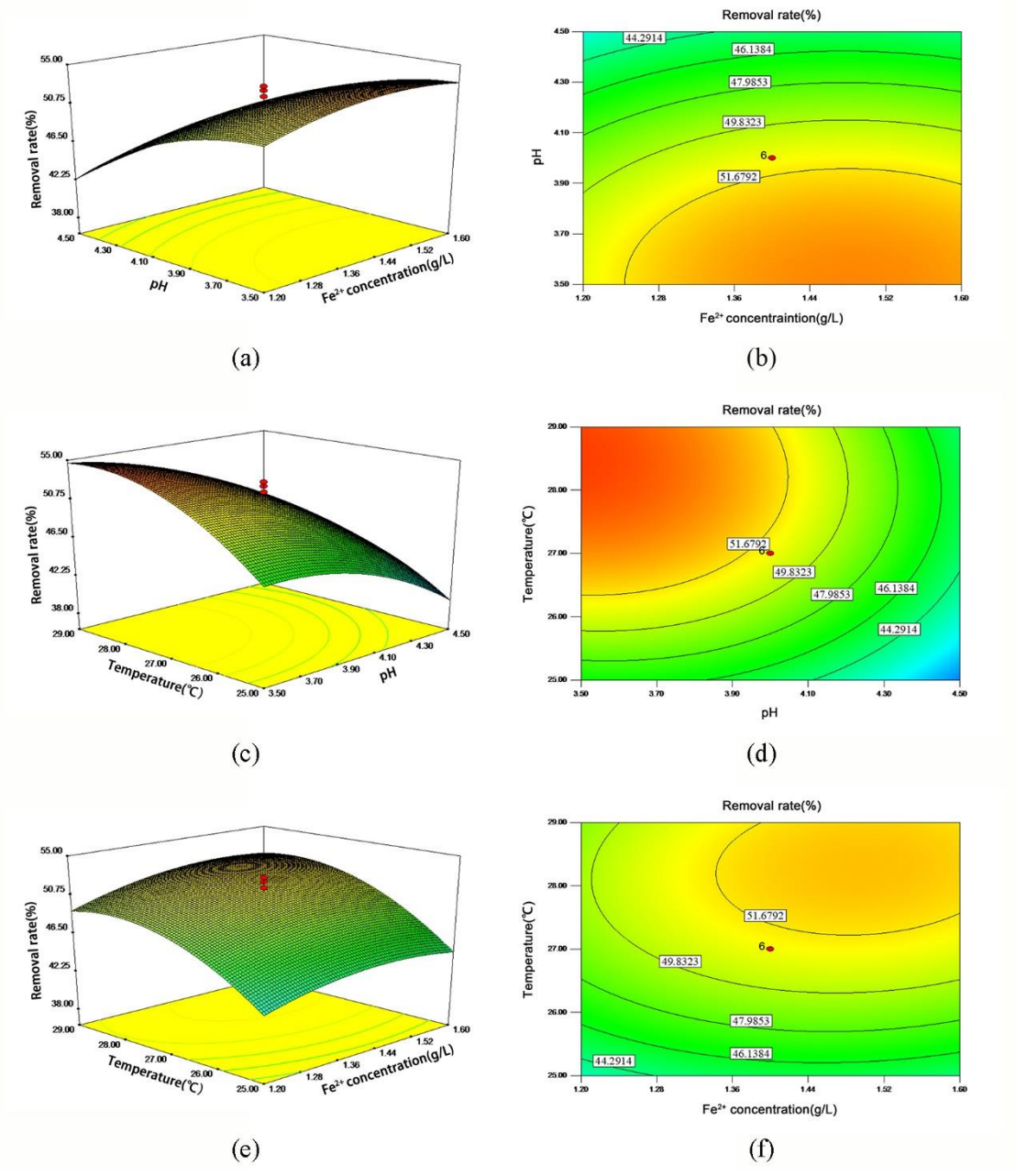
Removal rate(%)
55.00
50.75
46.50
42.25
38.00
pH
4.50
4.30
4.10
3.90
3.70
3.50
Fe2+ concentration(g/L)
1.20
1.28
1.36
1.44
1.52
1.60
(a)
Removal rate(%)
44.2914
46.1384
47.9853
49.8323
51.6792
6
pH
Fe2+ concentraintion(g/L)
(b)
Temperature(℃)
29.00
28.00
27.00
26.00
25.00
(c)
Removal rate(%)
51.6792
49.8323
47.9853
46.1384
44.2914
pH
Temperature(℃)
(d)
(e)
Removal rate(%)
51.6792
49.8323
47.9853
46.1384
44.2914
Fe2+ concentration(g/L)
Temperature(℃)
(f)

Fig. 3

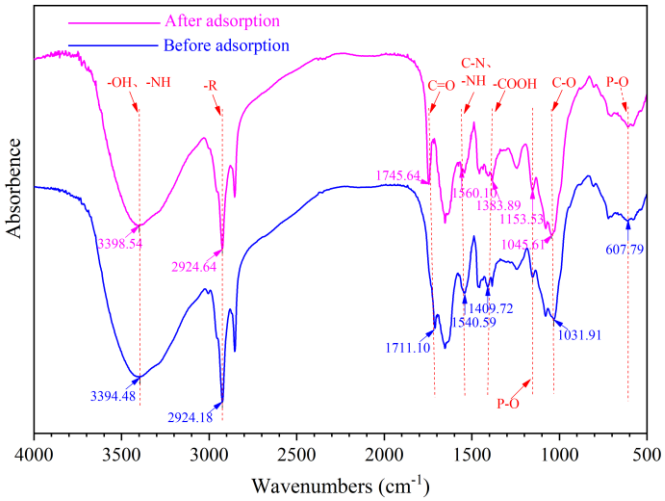
After adsorption
Before adsorption
-OH、-NH
-R
C=O
C-N、
-NH
-COOH
C-O
P-O
3398.54
2924.64
1745.64
1560.10
1383.89
1153.53
1045.61
607.79
3394.48
2924.18
1711.10
1409.72
1540.59
1031.91
P-O
Absorbence
4000
3500
3000
2500
2000
1500
1000
500
Wavenumbers (cm-1)

Fig. 4

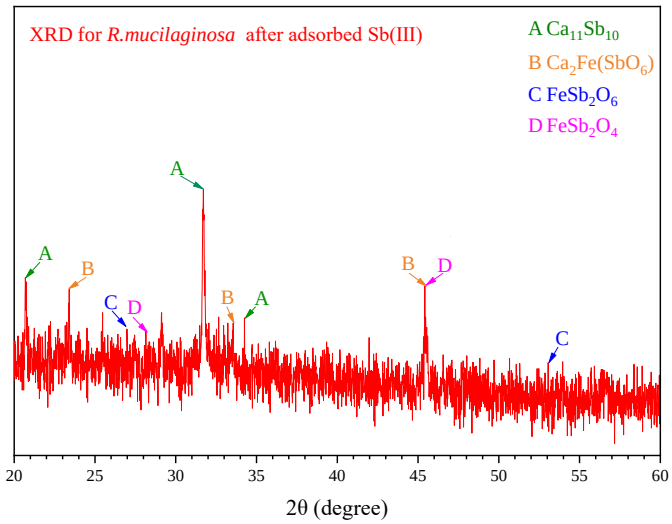
XRD for R.mucilaginosa after adsorbed Sb(III)
A Ca11Sb10
B Ca2Fe(SbO6)
C FeSb2O6
D FeSb2O4
A
A
B
C
D
B
A
B
D
C
20
25
30
35
40
45
50
55
60
2θ (degree)

Fig. 5

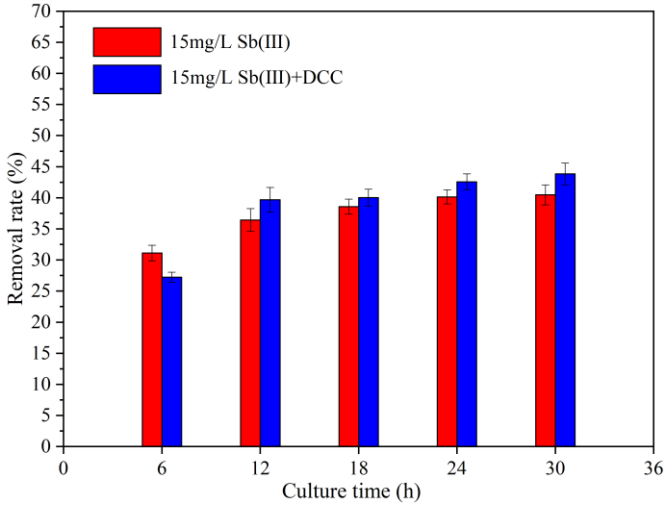
15mg/L Sb(III)
15mg/L Sb(III)+DCC
Removal rate (%)
Culture time (h)
0
5
10
15
20
25
30
35
40
45
50
55
60
65
70
0
6
12
18
24
30
36

Fig. S1: Some nutritional and environmental factors((a) carbon source concentration, (b) nitrogen source concentration, (c) inorganic salt, (d) agitation speed, (e)initial Sb(III) concentration) on Sb(III) biosorption

Fig. S2: SEM-EDS images of DJHN070401 before(a) and after(b) Sb(III) biosorption

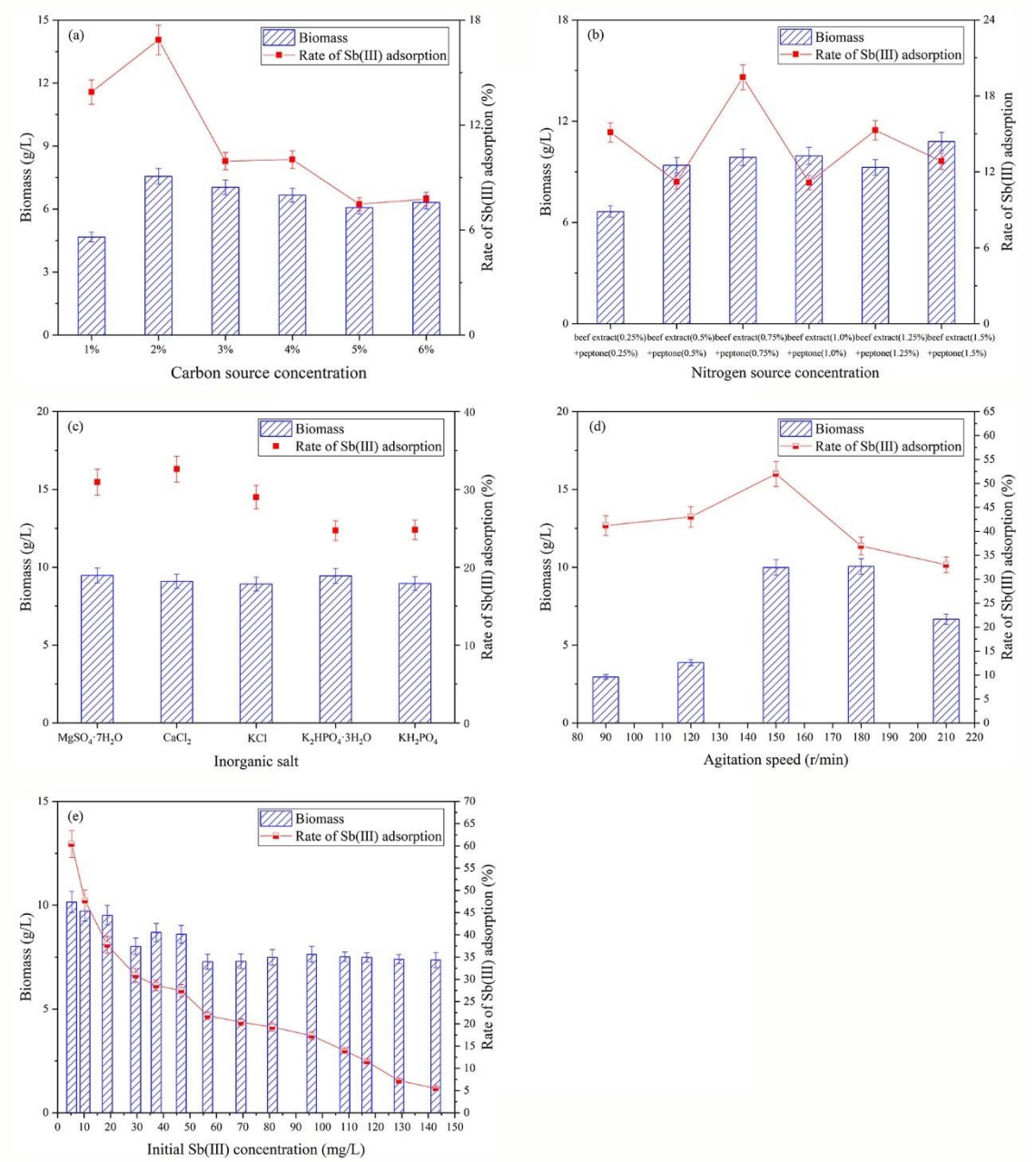

Fig. S1: Some nutritional and environmental factors((a) carbon source concentration, (b) nitrogen source concentration, (c) inorganic salt, (d) agitation speed, (e)initial Sb(III) concentration) on Sb(III) biosorption

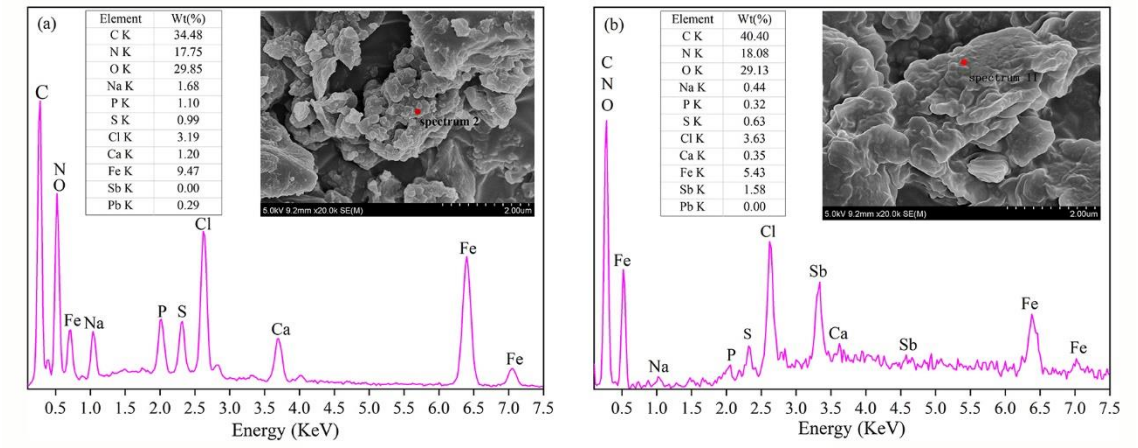

Fig. S2: SEM-EDS images of DJHN070401 before(a) and after(b) Sb(III) biosorption